Acta Crystallographica Section B
Structural Science
ISSN 0108-7681

Perchlorophenalenyl radical, $C_{13}Cl_9$: a modulated structure with nine threefold-symmetric molecules in the asymmetric unit

P. A. Koutentis,[a] R. C. Haddon,[a] R. T. Oakley,[b] A. W. Cordes[c] and C. P. Brock[a]*

[a]Departments of Chemistry and Physics and the Center for Advanced Carbon Materials, University of Kentucky, Lexington, KY 40506-0055, USA, [b]Department of Chemistry, University of Waterloo, Waterloo, Ontario, Canada N2L 3G1, and [c]Department of Chemistry and Biochemistry, University of Arkansas, Fayetteville, AR 72701, USA

Correspondence e-mail: cpbrock@pop.uky.edu

Received 20 November 2000
Accepted 10 July 2001

The odd-alternant perchlorophenalenyl radical, $C_{13}Cl_9$, forms molecular stacks centered on crystallographic threefold rotation axes, but the spacing within the stacks (3.78 Å) is too large to allow good overlap of the orbitals in which the spin density is localized. The radical is ruffled because of the intramolecular repulsions between α Cl atoms (the Cl···Cl *peri* interactions); the average displacement of an α Cl atom from the molecular plane is ~0.7 Å. The deviations from molecular planarity do not, however, determine the spacing within the stacks, which is determined instead by interactions between stacks. The modulations found in the *P*3*c*1 superstructure are a response to the short interstack contacts that would occur in the average pseudocell structure ($R\bar{3}m$, $\mathbf{c}' = \mathbf{c}/6$). The primary modulation is a pattern of enantiomeric alternation; a secondary modulation involves small rotations of the molecules around their threefold axes. The number (9) of independent molecules in the true cell is exceptionally large because of the conflict between the preference within the molecular stacks for threefold rotational symmetry and the preference in directions perpendicular to the stack axes for twofold alternation of enantiomers. The structural complexity reduces the precision of the distances and angles determined, but the average values found are in excellent agreement with those calculated by density functional theory.

1. Introduction

Odd-alternant hydrocarbons in general, and phenalenyl radicals in particular, have been suggested (Haddon, 1975*a*,*b*) as possible organic metals. The perchlorophenalenyl radical, $C_{13}Cl_9$, was an especially attractive synthetic target (Haddon *et al.*, 1987; Koutentis *et al.*, 2001) because the peripheral Cl atoms were expected to protect the radical from dimerization.

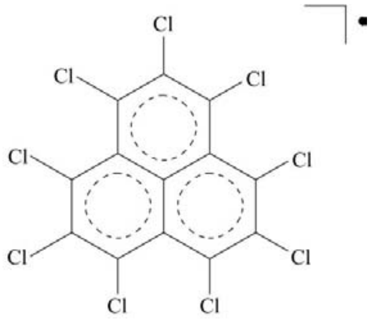

Table 1
Reflection statistics.

Condition	Number of unique reflections	$I > 2\sigma(I)$	$I > 10\sigma(I)$
$\ell = 6n$ $[\mathrm{mod}(\ell,6) = 0]$	1906	60%	31%
$\ell = 6n \pm 1$ $[\mathrm{mod}(\ell,6) = 1; 5]$	3180 (1590; 1590)	58% (58%; 58%)	29% (29%; 29%)
$\ell = 6n \pm 2$ $[\mathrm{mod}(\ell,6) = 2; 4]$	3340 (1920; 1920)	58% (57%; 58%)	21% (22%; 21%)
$\ell = 6n + 3$ $[\mathrm{mod}(\ell,6) = 3]$	1598	60%	14%
$\ell = 6n$; $\mathrm{mod}(-h + k - \ell,3) = 0$	632	98%	89%
$\ell = 6n$; $\mathrm{mod}(-h + k - \ell,3) \neq 0$	1274	20%	1%

Both older (Haddon, 1975*b*) and more recent (this work) quantum-mechanical calculations show that the HOMO of the $C_{13}Cl_9$ radical is nondegenerate and has threefold rotational symmetry, that the bond lengths change little when the radical is oxidized to the cation or reduced to the anion, and that the disproportionation energy of the radical (*i.e.* the energy difference between the cation and anion) is small. The small disproportionation energy favors delocalization of electrons. The threefold symmetry should favor the formation of molecular stacks. The similarity of bond lengths in the cation, radical and anion means that delocalization can occur without much structural reorganization.

All of these expectations were fulfilled, but the material fails as a conductor because the distance between molecules within the stacks (*ca* 3.78 Å) is substantially larger than twice the van der Waals thickness for an aromatic system (2 × 1.70 = 3.40 Å) or twice the van der Waals radius for a Cl atom (2 × 1.80 = 3.60 Å; Pauling, 1960). The larger-than-expected spacing is a result of Cl···Cl interactions between adjacent stacks.

The crystal structure of $C_{13}Cl_9$ is unusually complex: there are nine independent molecules, each of which lies on a threefold rotation axis. The structure is a modulated superstructure; reflections with $\ell \neq 6n$ are systematically weak and refinement in a pseudocell that has $\mathbf{c}' = \mathbf{c}/6$ is quite successful. The modulations are a response to the interstack interactions. The tilting or slipping of molecules that might be expected, and that would almost certainly lead to a lower symmetry structure with a smaller number of independent molecules, is prevented in $C_{13}Cl_9$ by the molecular ruffling, which is caused by the *peri* interactions of the Cl substituents.

A preliminary report of the structure of the $C_{13}Cl_9$ pseudocell has appeared in another journal (Koutentis *et al.*, 2001).

2. Experimental

2.1. Crystals

Crystals of $C_{13}Cl_9$ were grown by sublimation at 423 K and 10^{-5} torr. They melt at 521 K under Ar and decompose in air at 433 K. The crystals grow as quite long prisms that are black and shiny. The six faces of the trigonal crystals described below belong to the form $\{11\bar{2}0\}$.

The scattering patterns of 23 crystals were examined with the Nonius CAD-4 diffractometer at the University of Arkansas and/or the Nonius KappaCCD diffractometer at the University of Kentucky. Nine of the 23 diffraction patterns indexed to give a trigonal/hexagonal cell with $a \simeq 18.70$ and $c \simeq 22.68$ Å; the other 14 presented a variety of problems. The peaks for some of the crystals in the latter group were very broad; the peaks for others were narrow, but could not be indexed. For some crystals the indexing procedure gave a smaller unit cell [$c \simeq (22.68$ Å$)/6$] that left many peaks with non-integral indices. The indexing problems were no surprise because many of the crystals were obvious intergrowth twins.

All crystals but one were examined at room temperature. The diffraction pattern of the one crystal that was cooled did not change between *ca* 296 and 173 K, but the crystal shattered when returned to room temperature. We decided against examining other crystals at low temperature because cooling is much more likely to increase the size of the unit cell than to reduce it. We also feared losing the one phase-pure crystal we had finally found.

2.2. Data

Full sets of data for two crystals were collected at room temperature on the Nonius KappaCCD diffractometer at the University of Kentucky. Frames were measured with graphite-monochromated Mo *Kα* radiation (λ = 0.71073 Å) under control of the program *COLLECT* (Nonius, 1999). The data collected were highly redundant (13 different scan sets for a total of 1475 1° frames for the second crystal). Cells were determined and the data reduced with *DENZO-SMN* (Otwinowski & Minor, 1997). No absorption correction (other than the correction implicit in the scaling procedure) was made because the crystal, which was nearly equidimensional in cross section, had been mounted with the prism axis approximately parallel to the goniometer axis φ.

After the orientation matrices had been determined the information in the frames was transformed using the routine *PRECESSION* in *COLLECT* to give undistorted views of slices $nk\ell$ and $hn\ell$, $n = 0$–3, and hkn, $n = 0$–24, of the reciprocal lattice. These slices show that the diffraction pattern of the second crystal is ‘clean’. The diffraction pattern for the first crystal, however, is contaminated by the pattern from a

Table 2
Experimental details.

	Full structure	Pseudocell refinement
Crystal data		
Chemical formula	$C_{13}Cl_9$	$C_{13}Cl_9$
Chemical formula weight	475.18	475.18
Cell setting, space group	Trigonal, *P*3*c*1	Trigonal, *R*3*m*
a, c (Å)	18.704 (3), 22.675 (4)	18.704 (3), 3.7792 (7)
V (Å^3)	6870 (2)	1145.0 (3)
Z	18	3
D_x (Mg m^{-3})	2.067	2.067
Radiation type	Mo $K\alpha$	Mo $K\alpha$
No. of reflections for cell parameters	63 143	63 143
θ range (°)	1.3–27.5	1.3–27.5
μ (mm^{-1})	1.64	1.64
Temperature (K)	299 (1)	299 (1)
Crystal form, color	Prism, black	Prism, black
Crystal size (mm)	0.40 × 0.10 × 0.10	0.40 × 0.10 × 0.10
Data collection		
Diffractometer	Nonius KappaCCD	Nonius KappaCCD
Data collection method	φ and ω scans with 1.0° steps	φ and ω scans with 1.0° steps
Absorption correction	Multi-scan	Multi-scan
$T_{\min}$	0.79	0.79
$T_{\max}$	0.85	0.85
No. of measured, independent and observed parameters	40 131, 10 524, 6178	2409, 323, 318
Criterion for observed reflections	$I > 2\sigma(I)$	$I > 2\sigma(I)$
$R_{\rm int}$	0.033	0.034
$\theta_{\max}$ (°)	27.5	27.5
Range of h, k, l	$0 \rightarrow h \rightarrow 24$ $-21 \rightarrow k \rightarrow 0$ $-29 \rightarrow l \rightarrow 29$	$0 \rightarrow h \rightarrow 24$ $-21 \rightarrow k \rightarrow 0$ $-4 \rightarrow l \rightarrow 4$
Refinement		
Refinement on	F^2	F^2
$R[F^2>2\sigma(F^2)]$, $wR(F^2)$, S	0.094, 0.174, 2.15	0.045, 0.14, 4.08
No. of reflections and parameters used in refinement	10 524, 448	323, 64
Weighting scheme	$w = 1/[\sigma^2(F_o^2) + (0.030P)^2]$, where $P = (F_o^2 + 2F_c^2)/3$	$w = 1/[\sigma^2(F_o^2) + (0.030P)^2]$, where $P = (F_o^2 + 2F_c^2)/3$
$(\Delta/\sigma)_{\max}$	0.001	0.000
$\Delta\rho_{\max}$, $\Delta\rho_{\min}$ (e Å^{-3})	0.55, −0.44	0.36, −0.33

second, much smaller, crystallite that has $c \simeq (22.68$ Å$)/6$ and slightly different values of a and b.[1] Data from the first crystal were used for structure solution and initial refinement, but all analyses and refinements reported below are for the second crystal.

There was no sign in either set of frames of significant diffuse scattering. We saw no sign of any incommensurate modulation.

Inspection of the 'precession pictures' showed immediately that the crystal structure is a modulated superstructure. The fraction of reflections having $I > 10\sigma(I)$ (see Table 1) is largest for layers $hk\ell$, $\ell = 6n$ and $6n \pm 1$, is smaller for layers with $\ell = 6n \pm 2$, and is smallest for layers with $\ell = 6n + 3$. The modulation is large enough, however, that the fraction of 'observed' reflections $[I > 2\sigma(I)]$ is about the same (*ca* 60%) for all the layers.

The absence condition for rhombohedral centering is obeyed almost perfectly for the $\ell = 6n$ reflections (see Table 1). The nearly exact R centering in the pseudocell structure ($\mathbf{c}' = -\mathbf{c}/6$) is responsible for the low fraction of $\ell = 6n$ reflections that have $I > 2\sigma(I)$. There is no evidence of centering in the superstructure.

Wilson plots for the classes of reflections shown in Table 1 (see Xia *et al.*, 2001) are included with the supplementary material. They show that at $\theta = 13°$ the ratios of the average normalized intensities of the $\ell = 6n \pm m$, $m = 0, 1, 2$ and 3, reflections are 80:80:15:1. At that same scattering angle the average normalized intensity of the $\ell = 6n$ reflections that obey the R-centering condition is 330 times larger than for the $\ell = 6n$ reflections that do not. The latter ratio, however, is reduced to 90 at $\theta = 25°$, because the small differences between pseudosymmetrically related molecules become more important as the scattering angle increases.

All reflections $h0\ell$, $\ell \neq 2n$, seem to be extinct. We found no other pattern of absences in either the pseudocell or supercell reflections.

2.3. Structure solution

The basic arrangement of the molecules in the unit cell could be determined from the trigonal symmetry, the approximate rhombohedral centering and the cell dimensions. Solution of the full structure, or even of the pseudocell structure having $c' = c/6$, proved more difficult, partly because the extra scattering (data from the first crystal) interfered with the identification of space-group absences. Eventually the full structure was solved in the noncentrosymmetric space group *P*3*c*1 (No. 158) using the program *SIR*92 (Altomare *et al.*, 1994) in the program suite *maXus* (Mackay *et al.*, 1998). The corresponding centrosymmetric group, $P\bar{3}c1$ (No. 165), would require that at least 1/3 of the molecules be disordered across inversion centers. There are nine independent molecules in the asymmetric unit, each of which is located on a threefold rotation axis. The molecules are organized into three stacks

---

[1] The *PRECESSION* projections for the *hk*5, *hk*6 and *hk*7 layers of the two crystals are included in the supplementary material. Supplementary data for this paper are available from the IUCr electronic archives (Reference: BS0014). Services for accessing these data are described at the back of the journal.

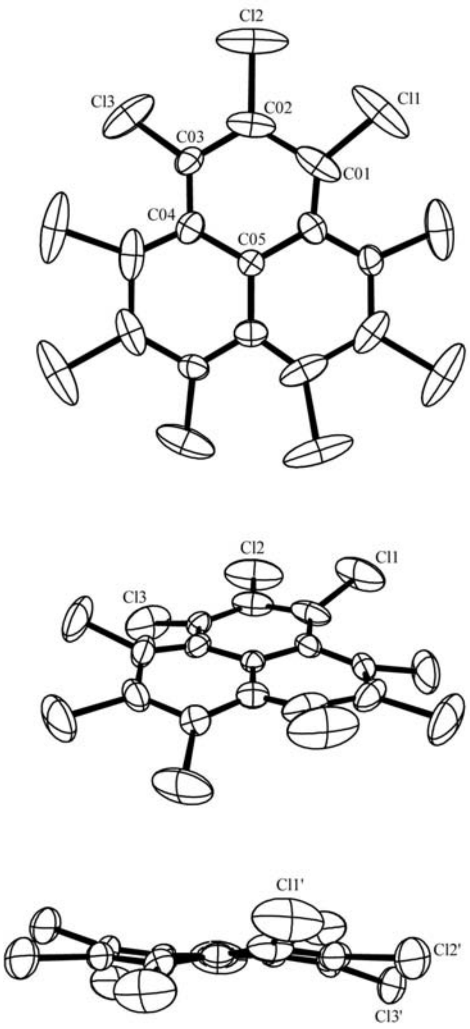

Figure 1
Perspective drawings of the molecular structure of $C_{13}Cl_9$, as determined in the pseudocell refinement. The shapes of the ellipsoids correspond to 50% probability contours of atomic displacement and the atom-numbering scheme is shown. The two lower drawings are rotated around the horizontal by 60 and 90° relative to the top drawing. The symmetry operation for the atoms marked in the lowest drawing is $2-x+y, 1-x, z$.

that lie on the three independent rotation axes. The second and third stacks are offset by $\Delta z \simeq \pm 1/18$, *i.e.* by ±1.26 Å. One of the nine molecules appeared from the first stages of structure solution to be disordered over two sites having similar occupancies.

2.4. Refinement in the pseudocell

The pseudocell structure is derived from the *P*3*c*1 structure by the transformation $\mathbf{a}' = \mathbf{a}$, $\mathbf{b}' = \mathbf{b}$ and $\mathbf{c}' = -\mathbf{c}/6$ [c' = 3.7792 (7) Å] and is in space group *R*3*m* (No. 160). The molecules have threefold rotational symmetry and also appear to be disordered across the mirror planes, which are the projections of the *c* glide planes of group *P*3*c*1. Atom C01 lies so close to the mirror that the refinement is unstable unless C01 is constrained to lie on the plane. The reference molecule of the *R*3*m* structure corresponds to molecule *G* of the *P*3*c*1 structure (see below), except that *z* is replaced by $-z$.[2]

Refinement of the pseudocell structure was straightforward and, perhaps even disturbingly, satisfactory (see Table 2). The distances and angles, which are determined for averaged atomic positions, are much more precise than they are accurate [*e.g.* C01—C02 1.587 (13) Å, but C02—C03 1.470 (15) Å; C03—C04 1.381 (12) Å, but C01—C04$(2-x+y, 1-x, z)$ 1.307 (9) Å]. The atomic ellipsoids, like the bond lengths, show the effects of inappropriate averaging, but are surprisingly reasonable (see Fig. 1). The molecule is not at all planar.

Note that the ratio of observations to variables in this refinement is exceptionally low, even though all data (averaged in $R\bar{3}m$) to $\theta = 27.5°$ were included. First, the space group is noncentrosymmetric. We could have left the Friedel reflections unaveraged, but it is not clear that the differences between the members of the Friedel pairs are significant, even when the full structure is refined (see below). Second, the apparent mirror nearly halves the number of unique data, but affects the number of variables only slightly. Finally, the molecule is very compact and contains no H atoms. If H atoms were present they would increase the size of the unit cell, and hence the number of independent reflections, without increasing the number of variable parameters. We could have applied numerous restraints, but the effects of averaging the molecules that are independent in the full structure would then have been obscured.

Refinement in the centrosymmetric $R\bar{3}m$ (No. 165) pseudocell that would be required if the space group were $P\bar{3}c1$ was unsuccessful (*R* on $F > 0.25$). The failure of the refinement in $R\bar{3}m$ supported the choice of space group *P*3*c*1 over group $P\bar{3}c1$.

2.5. Refinement in the *P*3*c*1 cell

The main differences between the superstructure and the pseudocell structure are the pattern of enantiomeric alternation and the small rotations (see Fig. 2) of the molecules around their threefold axes. There is also disorder at three of the nine sites; one disorder site was obvious at the time of structure solution and the other two became evident later. The model obtained from *SIR*92 (Altomare *et al.*, 1994) proved a good starting point; the relative rotations of the molecules all seem to have been correct. The challenge was to find a refinement model having an appropriate balance of degrees of freedom, constraints and restraints. We found the various options available in the least-squares program *SHELXL*97 (Sheldrick, 1997) invaluable.[3]

---

[2] This difference arises because the C05 atoms (see Fig. 1) that are separated by $\Delta x = -1/3$, $\Delta y = +1/3$, $\Delta z = +2/18 = +1/9$ in the *P*3*c*1 superstructure are separated by $\Delta x = -1/3$, $\Delta y = +1/3$, $\Delta z = 2/3$ (or $-1/3$) in the *R*3*m* structure. The standard symmetry operators for rhombohedral centering require that Δz is +1/3 if Δx, Δy is $-1/3$, +1/3.

[3] Other crystallographers would have chosen to refine the structure with a program that treats modulations explicitly. We believe that the highly restrained refinement reported here is reliable (see Table 2) and that there is no important disadvantage to characterizing the modulations after, rather than during, the least-squares refinement.

The basic atom-numbering scheme is the same for all molecules (see Fig. 1); the specific molecule is designated by a letter (*A*–*H*; *J*; see Figs. 2 and 3) at the end of the atom name.

Disorder at three sites (*E* with occupancy factor *ca* 0.50; *B* and *H* with occupancy factors *ca* 0.75) was included in the model. The C atoms for the two molecules at site *E*, and for both the Cl and C atoms of the minor components at sites *B* and *H*, were treated as rigid groups that pivot on atoms C05. The rigid groups were all based on the molecule at site *A*, which shows no sign of disorder. At first all three occupancy factors were varied, but the refinements converged very poorly, tended to drift and were sensitive to the starting values of the occupancy factors, which were highly correlated with each other and with the displacement parameters. Eventually we became convinced that there were good structural reasons (see below) for setting the occupancy factors at site *E* to 0.5 and for setting the occupancy factors for sites *B* and *H* equal [final value 0.76 (1)]. Doing so stabilized the refinement.

The final model included instructions (*DFIX*) restraining the five sets of chemically equivalent C—C and C—Cl bonds to have equal lengths (effective standard uncertainty 0.02 Å). The lengths of the five bond types were treated as variable parameters. The lengths of the two sets of Cl···C 1,3 distances (effective s.u. 0.06 Å) and of the four sets of C···C 1,3 distances (effective s.u. 0.04 Å) were restrained to be equal (*SADI* instructions). Instructions *FLAT* (effective s.u. 0.1 Å^3) were applied to the C05 and three C04 atoms in each of the independent molecules in an attempt to keep the C05 atoms in the planes defined by the attached C04 atoms. The nine molecules are so similar near their threefold axes that allowing the nine C04–C05 vectors to be different makes the refinement unstable.

The displacement parameters for the five sets of corresponding C atoms (*e.g.* C01*A*, C01*B*, ..., C01*J*) in the 12 molecules (six ordered and three disordered molecules) were constrained (*EADP*) to be equal; there is not enough information available about how the displacement ellipsoids differ for a stable or robust refinement in which all the C-atom U^{ij} parameters are varied. One *EADP* instruction could be used for all 12 C05 atoms, but two *EADP* instructions (six molecules in each) had to be used for the atoms C01–C04 because the orientations of the reference molecules, which were

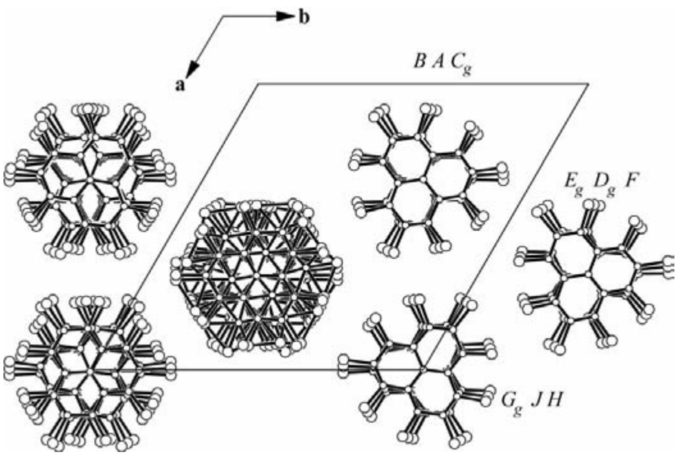

Figure 2
Projection of the supercell showing both complete and incomplete molecular stacks. The disorder of the *E* molecule is shown in the complete, but not in the incomplete, stack. Molecular labels are nearest the Cl1 atoms; the label C_g signifies that molecule *C* has been taken through a glide operation.

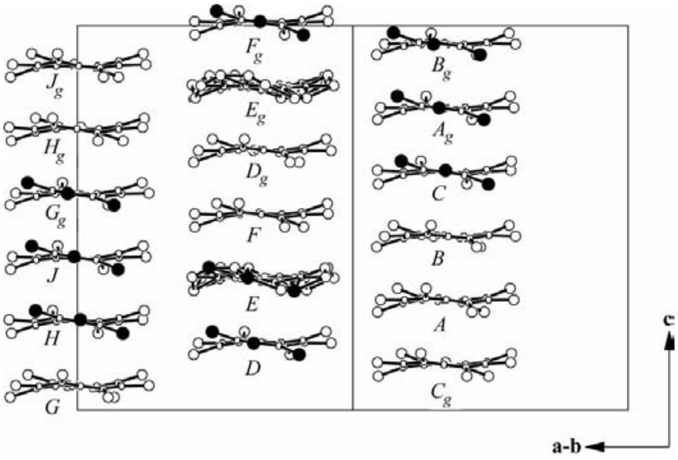

Figure 3
Projection of a slice of the supercell; the slice includes the vector **a**–**b**. The origin of the **c** axis is in the middle of the drawing. Molecules are labelled; the label C_g signifies that the molecule *C* has been taken through a glide operation. The disorder at site *E* is shown, but the disorders at sites *B* and *H* are not. The Cl atoms pointing out of the plane of the paper have been darkened (except for those of molecule *E*′).

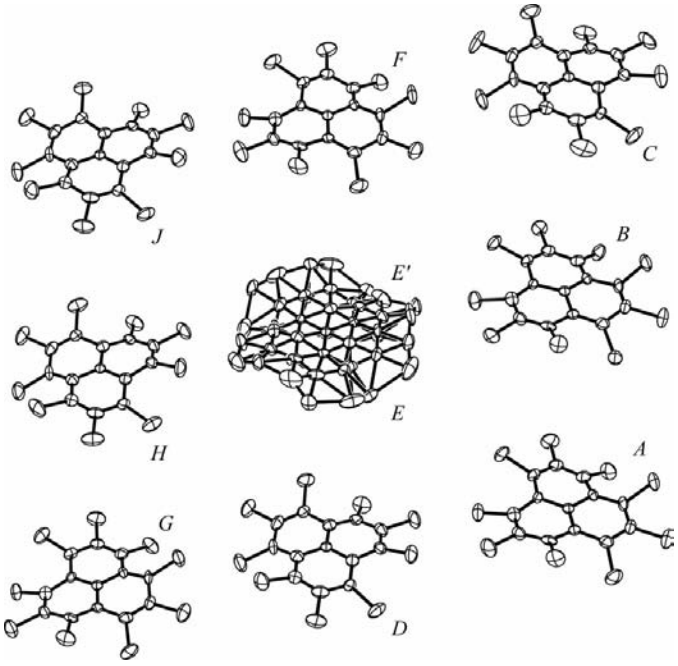

Figure 4
Perspective drawings of the individual molecules of the superstructure of $C_{13}Cl_9$. The shapes of the ellipsoids correspond to 50% probability contours of atomic displacement. The molecular labels are nearest the Cl1 atom of each molecule; the labels for the other atoms can be deduced from Fig. 1.

Table 3
Bond lengths (Å) calculated using *ab initio* density functional theory.

	C01—C02	C03—C04	C04—C05	C01—H; C01—Cl	C02—H; C02—Cl
$C_{13}H_9^+$, $D3h$	1.394	1.417	1.422	1.086	1.084
$C_{13}H_9$, $D3h$	1.392	1.418	1.431	1.086	1.086
$C_{13}H_9^-$, $D3h$	1.392	1.422	1.444	1.088	1.091
Δ(anion − cation)	−0.002	0.005	0.021	0.002	0.007
$C_{13}Cl_9^+$, $D3h$	1.402	1.439	1.454	1.718	1.729
$C_{13}Cl_9$, $D3h$	1.398	1.436	1.461	1.742	1.742
$C_{13}Cl_9^-$, $D3h$	1.392	1.434	1.471	1.765	1.759
Δ(anion − cation)	−0.010	−0.005	0.017	0.047	0.030
$C_{13}Cl_9^+$, $D3$	1.404	1.433	1.438	1.716	1.724
$C_{13}Cl_9$, $D3$	1.402	1.425	1.439	1.734	1.732
$C_{13}Cl_9^-$, $D3$	1.394	1.426	1.446	1.760	1.760
Δ(anion − cation)	−0.009	−0.008	0.008	0.045	0.036

chosen to give a compact unit with the most disordered molecule in the center, fall into two groups. The final atomic ellipsoids (see Fig. 4) show that these approximations are reasonable, but the use of *EADP* instructions for the Cl atoms, which are both more electron-rich and farther from the center of mass than the C atoms, proved unsatisfactory. Even if the librational, translational and internal vibrational motions were the same for all the molecules, as they probably are (at least approximately), the ellipsoids for the corresponding Cl atoms of two molecules separated by a rotation of *ca* 8° differ enough to matter. The displacement parameters for the minor components at sites *B* and *H* were set equal to those for molecules *C* and *G*, which have nearly the same orientations.

The values of wR (F^2) and S depend strongly on the weights chosen for the intensities. In the end we chose a very conventional scheme (see Table 2), even though it leads to a value of S that is above 2. The value of S for the full $P3c1$ structure can be reduced to 1.3 by using weights $w = 1/[\sigma^2(F_o^2) + (0.002P)^2 + 23P]$, where $P = (F_o^2 + 2F_c^2)/3$, in which case the agreement factors are 0.093 and 0.163.

The refined value of the Flack parameter (*TWIN* and *BASF* instructions) is 0.25 (9), which suggests significant inversion twinning. A refinement using data averaged in $P\bar{3}$ ($R_{\rm int}$ = 0.020) gave marginally better agreement factors (R_1 = 0.091; wR_2 = 0.172), but marginally poorer displacement ellipsoids. In the end we decided to leave in the description of the inversion twinning [$F(000) = 18\,(231 + 1.379 + 1.48\,i)$ e], but do not claim that it has any physical significance. We found no evidence of any obverse/reverse twinning. There was no indication that any extinction correction was needed.

The final agreement factors (see Table 2) are very satisfactory. The values of R_1 and wR_2 drop to 0.077 and 0.169 if $\theta_{\rm max}$ is lowered from 27.5 to 25.0°. The highest peak in the final difference map (0.55 e Å^{-3}) is located 0.05 Å from C05*B*, which suggests that the occupancy factor for C05*B* should actually be a little higher than for C05*H*. Other features (heights in the range +0.41 to −0.44 e Å^{-3}) suggest that there could be very minor disorder of molecules *C* and *G*, and possibly *F*. The only serious violation of the restraints are the displacements of atoms C10*B* (C05*B* for the minor component of molecule *B*) and C05*E* (one of the two components) from the planes of the three bonded C04 atoms (−0.71 and −0.35 Å; all other corresponding values are < 0.065 Å with individual s.u.'s of ~0.011 Å). Since the rigid groups used to describe these atoms included only one C04 atom, these rather large displacements may indicate that the disordered molecules are not quite aligned with the threefold rotation axes.

After the refinement was complete we checked again to be sure that the group $P3c1$ was a better choice than the centrosymmetric group $P\bar{3}c1$. Careful analysis of the small rotations of the molecules around their threefold axes (see below) confirmed that the molecule pairs that would be related by an inversion operation if the space group were $P\bar{3}c1$ (*A*/*J*, *B*/*H*, *C*/*G*, *D*/*F*, *E*/*E*′) are not related by any $\bar{1}$ operation. The differences in the rotations are small but systematic. In any event, an attempt to refine the structure in $P\bar{3}c1$ after shifting the origin by −0.667, −0.333, −0.333 was unsuccessful. The value of R_1 never went below 0.20, the atomic ellipsoids were physically unreasonable (much worse than those in Fig. 1) and there were large peaks (1.1–2.1 e Å^{-3}) in the difference Fourier map that suggested alternate molecular orientations for molecules *A*, *C* and *D*. The near centrosymmetry does, however, explain the instabilities in the refinement.

The input file for the final set of least-squares cycles is included with the supplementary material. Programs used to prepare material for publication included *SHELXTL/PC* (Sheldrick, 1990) and CIF-processing macros written locally.

3. Molecular geometry

Individual molecules of $C_{13}Cl_9$ are strongly ruffled (see Fig. 1) because the Cl1···Cl3 contacts across the 'bays' (the Cl···Cl *peri* interactions) would be impossibly short if the molecule were planar. The van der Waals radius of a Cl atom is 1.80 Å (Pauling, 1960), but even with the out-of-plane distortions the three intramolecular Cl···Cl distances are only 2.99–3.06 Å. These distances are very similar to those seen in octachloronaphthalene (Herbstein, 1979, and references therein), in two crystal forms of decachloropyrene (Hazell & Jagner, 1976; Hazell, 1978), and in other structures of polychorinated aromatic hydrocarbons retrieved from the Cambridge Structural Database (Allen & Kennard, 1993; hereafter known as the CSD). The extent of ruffling can be described by the torsion angles across the molecular 'bay' [Cl1—C01···C03—Cl3; 30.6 (4)–36.0 (8)°] and by the displacements of the Cl atoms from the plane of the three C04 atoms [0.63–0.75 (1) Å for molecules with occupancy > 0.5]. The values of these parameters for $C_{13}Cl_9$ are comparable to those for the two other molecules cited above.

The average bond lengths and angles (see Fig. 5) are normal (Allen *et al.*, 1987; see also Herbstein, 1979). Herbstein (1979) has noted that the bond lengths in aromatic molecules are insensitive to Cl substitution and to out-of-plane deformation. There is, however, clear evidence of bond-angle strain in the 'bays'.

4. Comparisons with results of quantum mechanical calculations

Ab initio density functional theory calculations have been carried out at the B3LYP/6-31G** level for $C_{13}Cl_9$ and $C_{13}H_9$ using the *Gaussian*98 suite of programs (Frisch *et al.*, 1998). Geometry optimizations were performed within D_{3h} symmetry constraints for the $C_{13}H_9$ radical, cation and anion, and within both D_{3h} and D_3 symmetry constraints for the $C_{13}Cl_9$ radical, cation and anion (Table 3). Frequency calculations confirmed that true minima had been located. In the D_3 $C_{13}Cl_9$ cation, radical and anion the pitch angles τ[4] are 8.1, 8.5 and 8.4°.

The calculated and observed C—C distances agree better than could be expected. The observed C—Cl distances are a little shorter than the calculated values, but the discrepancies would be much reduced if good corrections could be made for the greater thermal motion of the Cl atoms.

A table showing the energies has been deposited. The stabilization energy that accompanies ruffling (or puckering) changes with the charge on the ring. The out-of-plane distortions stabilize the anion most (15.2 kJ mol^{-1}) and the cation least (6.1 kJ mol^{-1}). These trends can be attributed to the introduction of *s*-orbital character into the π-system as the distortion progresses (the curved carbon effect; Haddon, 1993). The disproportionation energy (IP-EA) is relatively constant (4.18 eV for D_{3h}, 4.14 eV for D_3 symmetry), because the IP (ionization potential) and EA (electron affinity) both increase as the ring system becomes more nonplanar. The IP and EA values parallel the results of the electrochemical measurements on $C_{13}H_9$ (IP = 6.07 eV, EA = 0.84 eV for D_{3h} symmetry) and $C_{13}Cl_9$ (IP = 6.95 eV, EA = 2.814 eV for D_3 symmetry); the latter is harder to oxidize and much easier to reduce (Haddon *et al.*, 1978; Koutentis *et al.*, 2001). Indeed, the gas phase data for $C_{13}Cl_9$ suggest it is a pseudohalogen.

A table showing calculated spin densities has also been deposited. The calculated hyperfine coupling constants for $C_{13}H_9$ are in reasonable agreement with the experimental values (Gerson, 1966). Spin density in $C_{13}Cl_9$ is concentrated on the α C atoms (C01 and C03). There is very little spin leakage onto the Cl atoms.

5. Analysis of the structure

5.1. Possible arrangements of molecular pairs

In a structure composed of free radicals the formation of dimers or of extended stacks is expected. Distances between the α C atoms (C01 and C03) of neighboring molecules should be relatively short to maximize the overlap of the unpaired spin density that is localized on these atoms.

The out-of-plane deformations of the $C_{13}Cl_9$ molecule place many restrictions on the spatial relationships of molecules adjacent in a dimer or stack. Two planar molecules related by translation along a mutual threefold axis would be in a favorable arrangement for overlap of spin density, but could not be closer together than about 3.45–3.50 Å (van der Waals radius of Cl is 1.80 Å; Pauling, 1960). Ruffling has few

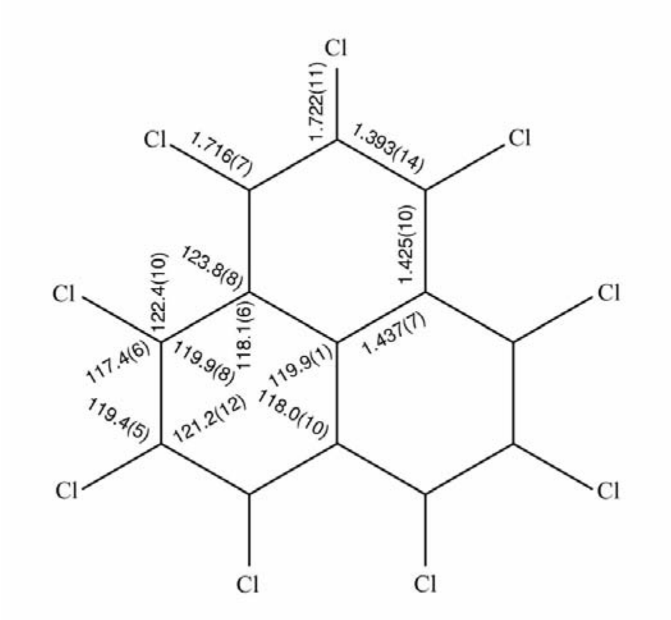

Figure 5
Bond lengths and angles averaged over the approximate *D*3 symmetry and over the eight independent molecules having occupancy factors > 0.5. The values in parentheses are the s.u.'s of the means.

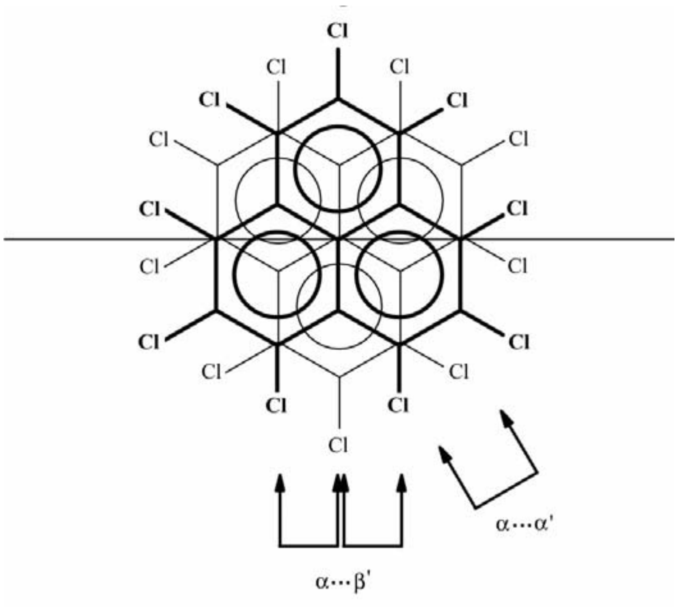

Figure 6
Line drawing showing the overlap when two molecules are related by a 60° rotation around the molecular threefold axis. The horizontal line is the trace of a glide plane that can relate the two molecules.

---

[4] The angle τ is defined as the dihedral angle between the plane of the atoms numbered here as C03, C04 and C05, and the plane of the atoms numbered C04, C05 and C04′, where atoms C04 and C04′ are related by the threefold rotation and all atoms are in the same six-membered ring

consequences for this arrangement because the out-of-plane displacements shift corresponding atoms of the two molecules in the same direction.

A second favorable arrangement couples translation along the threefold axis with a 60° rotation (atoms C01′ and C03′ over atoms C03 and C01; see Fig. 6). This arrangement is found in the structure of the 2,5,8-tri-*tert*-butylphenalenyl radical (Goto *et al.*, 1999), where the α (*i.e.* C01 and C03) substituents are H rather than Cl and the β (*i.e.* C02) subsituents are *tert*-butyl rather than Cl. This arrangement (see Fig. 6) has the advantage of minimizing steric repulsions between the β substituents, which are no longer superimposed when viewed down the threefold axis. The interplanar spacing in the structure of Goto *et al.* (1999) is about 3.2 Å.

The arrangement shown in Fig. 6, however, is incompatible with the close approach of two ruffled $C_{13}Cl_9$ radicals. The contacts between the α substituents on one molecule and the β substituents on an adjacent molecule would require the spacing to be at least 3.80 Å, *i.e.* 0.6 Å longer than in the Goto *et al.* (1999) radical.[5]

5.2. Stacks *versus* dimers

Translation-related, rather than glide-related (see Fig. 6), molecular pairs are expected for the $C_{13}Cl_9$ structure because the intermolecular distance in the former can be *ca* 0.35 Å shorter than in the latter.

There is nothing in the interaction of two $C_{13}Cl_9$ radicals that would interfere with propagation of either type of interaction along the threefold molecular axis. The $C_{13}Cl_9$ molecules have about the same thickness at the rim as in the center because the van der Waals radius (Pauling, 1960) for a Cl atom (1.80 Å) is nicely matched to the half thickness of an aromatic ring system (1.70 Å). The out-of-plane deformation of the $C_{13}Cl_9$ molecules retains the approximate symmetry 32 (or *D*3); the 'tops' and 'bottoms' of the molecules are therefore nearly the same. The tri-*tert*-butylphenalenyl radical (Goto *et al.*, 1999) packs very differently because the bulky β substituents must be bent away from the C-atom core when two molecules interact. This latter compound cannot form stacks, but forms dimers instead.

5.3. Retention of threefold symmetry

Retention of the threefold molecular axis requires that the atoms of molecules in stacks (or dimers) be superimposed in projection. There are not many compounds of simple, flat molecules that crystallize in this pattern (see Kitaigorodskii, 1961). Even fewer compounds form stacks of the type seen in $C_{13}Cl_9$. We have found only two comparison structures that are ordered: *s*-triazine (Coppens, 1967) and the solid-state compound of benzene with hexafluorobenzene (Overell & Pawley, 1982). Both compounds undergo phase transitions when cooled. The well studied transition in *s*-triazine ($C_3H_3N_3$; Coppens & Sabine, 1968; Prasad *et al.*, 1981, and references therein) involves a shear in the **a*****c** plane and rotation of the molecule around **b** as the space group changes from $R\bar{3}c$ to *C*2/*c*. Crystals of $C_6F_6{\cdot}C_6D_6$ undergo a series of phase transitions with cooling during which molecular rotational motion (as measured by NMR) is slowed and the molecules in the stacks are tilted relative to the stack axis (Williams *et al.*, 1992, and references therein).

There is additional evidence that a close-packed array of stacks having threefold rotational symmetry is characteristic of higher temperatures and greater thermal motion. Crystals of pentamethylcyclopentadienyllithium (stacks in which $C_5Me_5^-$ and Li^+ ions alternate) are rhombohedral at room temperature, even though location of the $C_5Me_5^-$ ions on threefold axes requires extensive disorder (Dinnebier *et al.*, 1999). This compound probably also undergoes a phase transition below room temperature, perhaps to the distorted hexagonal array of stacks (space group *Pnma*) found for cyclopentadienyllithium and cyclopentadienylsodium (Dinnebier *et al.*, 1997).

The ruffled perchlorophenyl radical is more likely than a more planar molecule to retain its threefold axis at room temperature and below. The tilting of planar molecules which are stacked has no consequence for the packing density of the stack and allows the edges of molecules in neighboring stacks to interleave in a favorable herringbone arrangement. The edges of the $C_{13}Cl_9$ molecule, however, are not perpendicular to the stack axis (see Fig. 3), so there is less to be gained by any reorientation. Furthermore, any tilt of the ruffled molecule relative to its threefold axis, or any offset of the molecules in a direction perpendicular to that axis, would lead to a significantly lower packing density. The modulations in the $C_{13}Cl_9$

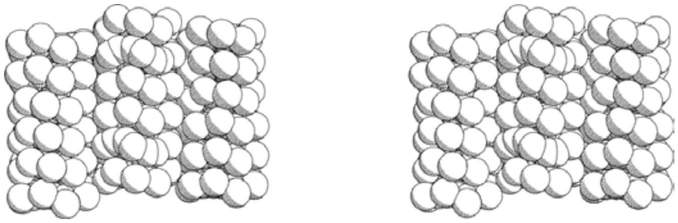

Figure 7

Stereoview of van der Waals surfaces (C, 1.6 Å; Cl, 1.8 Å) of the same set of molecules as shown in Fig. 3 (*i.e.* two asymmetric units related by a glide operation). In the stack at the far right the molecular chirality changes between the third and fourth molecules. In the stack at the far left the molecular chirality changes above the bottom molecule and again above the fourth molecule from the bottom. The disorder at site *E* is shown, but the disorders at sites *B* and *H* are not.

---

[5] In the dimer of Fig. 6 there are two types of important Cl···Cl interactions, $\alpha\cdots\alpha'$ and $\alpha\cdots\beta'$. The Cl···Cl distance within the plane of the projection is ~1.40 Å for each. If the minimum intermolecular Cl···Cl distance is to be at least 3.45 Å then the Cl···Cl separation parallel to the threefold axis may be no shorter than $[3.45^2 - 1.40^2]^{1/2}$ = 3.15 Å. Consider first the $\alpha\cdots\beta'$ contacts. One of the α Cl atoms must be displaced towards the β' Cl atom; the other must be displaced in the opposite direction. Since the refined structure shows that the out-of-plane displacements of the Cl1 and Cl3 atoms are about 0.65–0.70 Å, the intermolecular separation must then be at least 3.15 + 0.65 = 3.80 Å. The $\alpha\cdots\alpha'$ contacts add a further restriction: the operation relating the two molecules must result in the α and α' atoms being displaced in the same direction along the threefold axis. Since a 60° rotation coupled with a translation does not meet this requirement, the two molecules must be related by a glide operation (approximate or true) with the plane passing through (or near) C01 (or C03) and C05 (see Fig. 1 for atom-numbering scheme).

Table 4
Fraction of molecular pairs that are homochiral in superstructures having **c** = *n* (3.78 Å), see Figs. 9 and 10.

Intermolecular vector	(−1/3, +1/3, −1/(3*n*))	(−1/3, +1/3, +2/(3*n*))	(0, 0, 1/*n*)
n = 1 (**c** = 3.78 Å)	1	1	1
n = 2 (**c** = 7.558 Å)	0	1	0
n = 4 (**c** = 15.117 Å)	1/2	0	1/2
n = 6 (**c** = 22.675 Å)	4/9	1/9	2/3

structure probably substitute for the molecular tilting found in most related structures (see also below).

5.4. Arrangement of the stacks

The stacks form a hexagonally close-packed array (see Fig. 2). Each stack is surrounded by three adjacent stacks that are offset by *ca* +**c**/18 and three more that are offsert by *ca* −**c**/18 (see Figs. 3 and 7).

Within each stack a group of three molecules related by approximate translations **c**/6 = 3.78 Å is followed by a group of three molecules related to the first group by a true glide operation (*e.g.* $A\ B\ C\ A_g\ B_g\ C_g\ A\ B\ C$,...; see Figs. 3 and 7). Both translation-related pairs and glide-related pairs (see Fig. 6) are present; there are twice as many of the former as of the latter.

Note that the spacing along the threefold axis **c** [(22.675 Å)/6 = 3.78 Å] is the same to within 0.1 Å for all pairs. That distance is the same as the minimum spacing estimated for the glide-related pair (Fig. 6), but is much longer than the minimum spacing (*ca* 3.45 Å) estimated for the translation-related pair. It must be that the spacing in the **c** direction is determined by interactions between, rather than within, the stacks (see Fig. 7). The same must be true in the $C_6F_6{\cdot}C_6D_6$ crystal, where the interplanar spacing is 3.62 Å, *i.e.* 0.2 Å longer than estimated from the sum of the van der Waals radii, and in *s*-triazine, where the spacing is 3.64 Å.

5.5. Alternation of enantiomers

When trying to understand this very complicated structure we found it informative to look at the simplest possible pseudocell structure, which would be in space group *R*3 (No. 146; see Fig. 8). This structure, which is derived from the *R*3*m* pseudocell structure by removing the mirror planes, is composed of translation-related stacks of molecules. Even if the separation within the stacks were as long as 3.78 Å, which would not indicate much orbital overlap, all Cl atoms would be involved in two impossibly short (< 3.3 Å) interstack contacts (see Fig. 8). These contacts would involve molecules that are related by the *R*-centering along the long diagonal of the rhombus (**a**–**b**) and along the two symmetry-related directions. The $\mathrm{Cl1}\cdots\mathrm{Cl3^{ii}}$ contact would involve atoms separated by 2**c**/3 [$\mathrm{Cl1}\cdots\mathrm{Cl3^{ii}}$ of 3.27 (1) Å; (ii) $\frac{2}{3}-y, x-y-\frac{2}{3}, z-\frac{2}{3}$] and the $\mathrm{Cl2}\cdots\mathrm{Cl2^{i}}$ contact would involve atoms separated by **c**/3 [$\mathrm{Cl2}\cdots\mathrm{Cl2^{i}}$ of 3.26 (1) Å; (i) $\frac{2}{3}-y, x-y-\frac{2}{3}, z+\frac{1}{3}$]. Any rotation of the molecule around its threefold axis that might relieve these specific contacts would generate other short contacts. It is not possible to make a densely packed structure of $C_{13}Cl_9$ molecules in *R*3 with *Z*′ = 1/3. Either the threefold symmetry must be lost or the number of independent molecules must be increased.

All short Cl···Cl contacts along **a**–**b** could be relieved if stacks adjacent in this critical direction were enantiomeric. The $\mathrm{Cl2}\cdots\mathrm{Cl2^{i}}$ distance would then become longer than 3.60 Å and the $\mathrm{Cl1}\cdots\mathrm{Cl3^{ii}}$ distance would become 3.51 (1) Å. Strict enantiomeric alternation of stacks, however, is incompatible with trigonal symmetry. Each stack is equidistant [$a/3^{1/2}$ = 10.80 Å] from six other stacks, which are also separated by $\mathbf{a}/3^{1/2}$. If three of the stacks in the surrounding hexagon were composed of one enantiomer and the other three stacks were composed of the other enantiomer, then what should be the handedness of the stack in the center? This is the kind of crystal phase that is described by solid-state physicists as 'frustrated'.

We looked at possible schemes for alternation of enantiomers in trigonal unit cells (space group *P*3 or higher) and

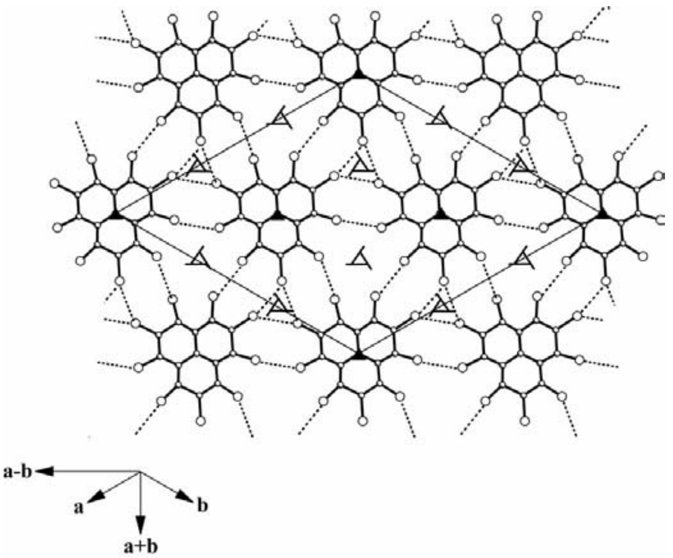

Figure 8
Projection of the pseudocell showing one of the two molecular orientations (effective space group *R*3 rather than *R*3*m*). The locations of the symmetry elements within one unit cell are shown. Three sets of the two short Cl···Cl contacts are marked. Note that the Δ*z* values for the contacts involving the Cl2 atoms have the opposite sign from the Δ*z* values for the contacts involving the Cl1 and Cl3 atoms. In projection the two sets of contacts seem to involve the same pair of molecules, but the contacts actually involve a molecule in one stack and two molecules in an adjacent stack.

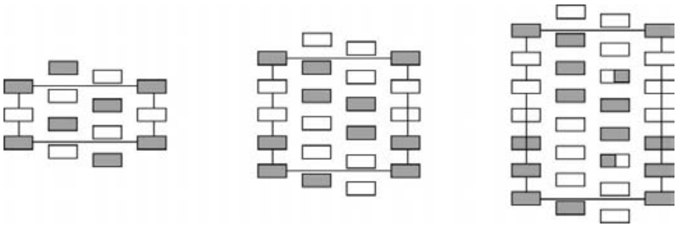

Figure 9
Diagrams showing possible schemes for enantiomeric alternation along −**a** + **b** (left to right) and **c** (upwards) in structures with *c* = *n* (3.78 Å), *n* = 2, 4 and 6.

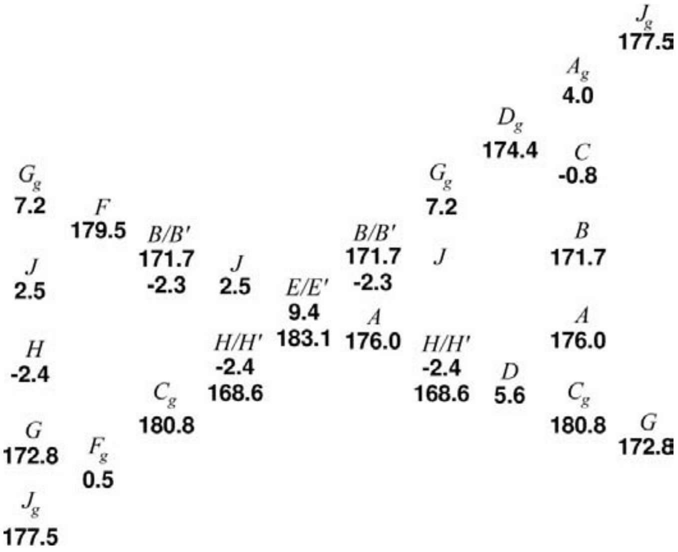

Figure 10
Diagram showing the angles φ [Cl2$\cdots$C05$\cdots$C05$(x, y, z+1)\cdots$C05$(x+1, y+1, z+1)$]. Values (s.u.'s < 0.1°) are displayed in the orientation of Fig. 3. The two diagonals are the two directions [$-\mathbf{a}/3$, $+\mathbf{b}/3$, $+\mathbf{c}/9$ and $\mathbf{a}/3$, $-\mathbf{b}/3$, $-\mathbf{c}/18$] in which the intermolecular contacts are structure determining.

compared them (see Fig. 9 and Table 4) with the basic arrangement found in the observed structure [disorder at sites *B* and *H* was ignored; all cells have *a* as found experimentally]. For each arrangement the number of homochiral pairs related by the approximate translations [$-\mathbf{a}/3$, $+\mathbf{b}/3$, $-\mathbf{c}/(3n)$], [$-\mathbf{a}/3$, $+\mathbf{b}/3$, $+2\mathbf{c}/(3n)$] and [0, 0, $\mathbf{c}/n$], where n is the value of c/3.78 Å, were counted. Perfect enantiomeric alternation for the $\Delta z \simeq 1/(3n)$ pairs gives a structure with $n = 2$ that has no alternation at all for the $\Delta z \simeq 2/(3n)$ pairs. Perfect alternation of the $\Delta z \simeq 2/(3n)$ pairs gives a structure with $n = 4$ that also has perfect alternation of the $\Delta z \simeq 1/(3n)$ pairs. The $n = 6$ structure is similar to the $n = 4$ structure, but 2/3 of the pairs within each stack are homochiral. Since it is the $n = 6$ structure that is actually found, it must be that having a greater fraction of homochiral (or translation-related) pairs within the stacks is important. Careful inspection of Fig. 7 supports this idea: a switch of chirality within a stack produces three short Cl$\cdots$Cl interactions and three small regions of empty space.

There is no other simple alternation pattern. If *a* and *b* are doubled then alternation can be perfect for one plane of homochiral stacks (*e.g.* the plane parallel to **a**–**b** and **c**), but a threefold rotation axis within any one of those stacks generates numerous homochiral pairs in other directions. The fundamental problem in this structure is the conflict between the drive for threefold rotational symmetry within the molecular stacks and the drive for twofold alternation of enantiomers in directions perpendicular to the stack axes.

In the observed $P3c1$ structure ($n = 6$) there are two symmetry-related sets of nine $\Delta z \simeq 2/(3n) = 2/18$ pairs (see Figs. 3 and 9). Since nine is an odd number the alternation of enantiomers cannot be perfect; there must be (at least) one 'mistake', *i.e.* one homochiral pair, for each set of nine pairs. That homochiral pair is localized in the vicinity of molecule *E*; pairs involved are $H\cdots E$, $E'\cdots B$, $C_g\cdots H'$ and $B'\cdots G_g$, where H' designates the minor component at site *H*. Since the structure has approximate inversion symmetry we expect the pair contacts on the two sides of molecule *E* to be very similar. If they are, the occupancy factors for the major components of *H* and *B* should be the same and the occupancy factor of *E* should be $\frac{1}{2}$, which constraint was applied during the refinement. Since the occupancy factor for *B* and *H* is close to $\frac{3}{4}$ [0.76 (1)], we believe that the unfavorable homochiral pairs are in fact distributed approximately equally across the four locations.

While the enantiomeric alternation makes *R* centering impossible, it generates the *c* glide plane of the superstructure. There are, therefore, three independent molecular stacks, each of which is composed of three independent molecules (see Fig. 3). Two of the three stacks (*ABC* and *GHJ*) are, however, very similar, and the third (*DEF*) is only a little different. The stacks *ABC* and *DEF* differ most in the relative rotations of the molecules around their threefold axes.

5.6. Rotational modulation

The rotations of the molecules around their threefold axes (see Fig. 2) are most easily understood by looking at the values of the angles in the projection down **c** (see Fig. 2) of the C05–Cl2 vectors with the vector **a** + **b**, which is the short diagonal of the unit-cell projection. These angles (hereafter, φ) are the torsion angles Cl2$\cdots$C05$\cdots$C05$(x, y, z+1)\cdots$C05$(x+1, y+1, z+1)$; values of φ describe the small rotations of the molecules around their threefold axes. The φ values are all near 0 or 180° and the angles for glide-related molecules must sum to 180°. Inspection of Fig. 3 shows that all molecules having φ near 0° are homochiral, as are all molecules having φ near 180°.[6]

The values of φ are all small: averages are 3.8 (1), 2.4 (1) and 3.1 (2)° for the *ABC*, *DEF* and *GHJ* stacks. The C05–Cl2 vectors of all molecules are nearly parallel to the short diagonal **a** + **b**. The relative rotations of homochiral molecules adjacent within a stack are 4–5°.

Along the diagonal $-\mathbf{a}/3$, $+\mathbf{b}/3$, $+\mathbf{c}/9$ (lower left to upper right of Fig. 10) there is alternation of molecular chirality except for the 'mistake' in the vicinity of molecule *E*. Along the diagonal $\mathbf{a}/3$, $-\mathbf{b}/3$, $-\mathbf{c}/18$ (upper left to lower right) the chirality changes after every second molecule except in the vicinity of molecule *E*.

The values of φ differ most from 0 and 180° at the disordered sites (especially H', E and B'); the deviations decrease with distance from *E* in the direction [$-\mathbf{a}/3$, $+\mathbf{b}/3$, $+\mathbf{c}/9$]. If a detailed analysis is made of the rotations of the individual molecules with respect to the average value for the corresponding stack the pattern is even clearer. This analysis included torsion angles φ calculated for atoms Cl1 and Cl3 as well as for Cl2. The average $\varphi' = \varphi - \langle\varphi\rangle$ stack values (s.u.'s $\leq$ 0.1° except for *E*, for which the s.u. is 0.2°) are then:

---

[6] Note that if the structure were in space group $P\bar{3}c1$ rather than $P3c1$ then the φ values for pairs *A*/*J*, *B*/*H* and *C*/*G* would differ by 180°, which they do not.

J_g (–0.1°); F_g (−2.5°); C_g (+4.6°); H (−4.7°); E (+6.4°); B (−4.4°); G_g (+4.6°); D_g (−2.4°); A_g (+0.1°); [J_g (−0.1°); F_g,...]. The corresponding deviations at the disordered sites (s.u.'s 0.2°) are:

H_g' (+8.9°); E_g' (−6.2°); B' (−5.9°).

The signs of the deviations alternate. The magnitudes of the deviations are largest near molecule E and smallest for the molecules farthest away.

We believe that the interactions between homochiral molecules separated by [−**a**/3, +**b**/3, +**c**/9] (lower left to upper right of Fig. 10) are most responsible for the rotational modulation. Interactions between homochiral molecules separated by [−**a**/3, +**b**/3, −**c**/18] (upper left to lower right of Fig. 10) and between heterochiral molecules within a stack may, however, also play a role. The structure is determined by a complicated balance of Cl···Cl repulsions.

6. Another crystal form?

We have seen a number of indications of a second crystal form that has a volume about 1/6th that of the $P3c1$ cell and one short cell constant that is very nearly (22.675 Å)/6.[7] The cell appears to have no threefold axis; rather, the diffraction patterns suggest tripling of a lower symmetry cell around a pseudo-threefold axis. This structure is likely to be similar to the $P3c1$ structure, but to have a different kind of modulation. Perhaps the molecules are tilted so that the molecular and crystallographic threefold axes are not quite parallel. The diffraction patterns that show this phase most clearly are so complicated that indexing might not be possible, even if the pure phase could be obtained. There seems to be rapid loss of order with scattering angle.[8]

The thermal-decomposition product of $C_{13}Cl_9$ is perchlorophenalenone, $C_{13}Cl_8O$. It is possible that the second phase includes this product or is nucleated by it.

7. Discussion

In the optimum crystal structure the molecular volume should be minimized, there should be good overlap of orbitals in which the spin density is localized and there should be no short intermolecular Cl···Cl interactions. All three conditions are important, but they cannot be satisfied simultaneously. The observed structure is a compromise that results in the number of independent molecules being exceptionally large (Brock & Dunitz, 1994).[9]

Stacks of interacting radicals can be formed without any problem. The molecules in these stacks would be expected to be homochiral because homochiral molecules can be substantially closer together than enantiomeric molecules (3.45 *versus* 3.80 Å).

Problems with Cl···Cl repulsions arise, however, when the stacks are arranged to fill space densely. The interstack Cl···Cl repulsions determine the spacing between molecules adjacent within a stack.[10] The interstack interactions coupled with the high symmetry also keep the intermolecular separations within the stacks even and so inhibit any transition involving a Peierls distortion.

The almost perfect alternation of enantiomers in the direction [−**a**/3, +**b**/3, +2**c**/18] seems to be the second important consequence of the interstack Cl···Cl repulsions. The conflict of this mod(2) requirement with the mod(3) requirement of the trigonal symmetry, and with the preference for enantiomerically pure stacks, leads to the $c = 6$ (3.78 Å) superstructure as well as to the major disorder at site E and the secondary disorders at sites B and H. The rotational modulation is almost certainly a response to the unfavorable contacts that are concentrated near site E, although the modulation may alleviate other packing problems as well.

Note that the $-T\Delta S$ contribution to the free energy of the observed structure is small because the disorder occurs at only a small number of sites. We estimate ΔS to be $(R/9)\ln 4 = 0.15R$ per mole of $C_{13}Cl_9$. At 523 K, the temperature at which the crystals were grown, the energy contribution from this disorder is estimated to be only 0.7 kJ mol^{-1}.

Why then is this structure so exceptional? First, there is the conflict between incompatible packing preferences that are similar in importance. The molecules should retain their threefold rotational symmetry, the molecules should form homochiral stacks and the chirality of molecules with centers related by the translation [−**a**/3, +**b**/3, +2**c**/18] should alternate. Second, the molecule is smaller and more rigid than most so that the importance of the packing problems is magnified. The surface/volume ratio is relatively large so that repulsive interactions are especially important (see Dunitz & Gavezzotti, 1999). The molecule has very little conformational flexibility and so cannot adapt easily to the requirements of a three-dimensional periodic arrangement. Most molecules can change a few torsion angles or deform a few bond angles to relieve repulsive intermolecular interactions, but $C_{13}Cl_9$ is relatively inflexible.

Note also that the small number of independent atoms makes detection of a complicated superstructure more likely. Since the average intensity varies with $(ZN_{\rm at})^{-1}$ (at least in the case of an equal-atom structure), the very weak superstructure reflections are much more likely to be noticed if $N_{\rm at}$ is small. The high proportion of electron-rich Cl atoms and the absence of electron-poor H atoms also raises the average intensity. Finally, use of a CCD diffractometer rather than of a serial

---

[7] See the *PRECESSION* projections (supplementary material) for the *hk*6 layer of the first crystal. The extra set(s) of spots are clearly visible.

[8] The indexing routine did find a trigonal cell with $c \simeq 3.8$ Å. The *PRECESSION* projections for the levels $\ell = 0, 1, 2$ and 3 of that cell are included with the supplementary material.

[9] There are only nine structures with $Z'' > 9$ and atomic coordinates in the October 2000 version (5.20) of the CSD. There is no structure with $Z' = 9\,(1/2) = 4.5$ or with $Z' = 9\,(1/3) = 3$.

[10] If the α Cl atoms were removed from $C_{13}Cl_9$ (to give $C_{13}H_6Cl_3$) the molecules would almost certainly be much more planar and the separation between two molecules might be reduced substantially. The effect of the interstack interactions involving β Cl atoms, however, is more difficult to predict; those interactions might still prevent the close approach of molecules that is required for good overlap of half-filled orbitals.

diffractometer increases the chances of noticing the very weak reflections characteristic of superstructures.

Finally, there is almost certainly an element of luck. If the modulations had had smaller amplitudes or longer periods they might simply have been seen as ‘thermal motion’ and/or ‘disorder’. If the packing problems had been more severe crystal growth might have been affected to the point that we would not have been able to measure a useful set of intensity data. The packing conflicts in this particular structure just happen to be satisfied (as well as possible) by modulations that can be observed and modeled. The structure of $C_{13}Cl_9$ may not be as exceptional for its complexity as it is for the possibility of observing and understanding that complexity.

So what then has been learned? First, that complex molecular structures can be refined and understood using techniques standard for small-molecule crystallography. Second, that the balance of forces and energies in crystals can be, and often is, exceptionally subtle. That the balance of forces and energies can be very subtle is well known to those who study modulated structures, incommensurate structures and complex sequences of phases (see van Smaalen, 1995). While neither of these observations is new, they are worth repeating.

This structure is also another counterexample to the common expectation that a simple molecule should crystallize in a simple structure. Other counterexamples are CBr_4 (*C*2/*c*, $Z' = 4$; More *et al.*, 1977) and pyridine (*Pna*2$_1$, $Z' = 4$; Mootz & Wussow, 1981). In fact, it may be the reverse statement that is true. Small molecules have fewer low-energy degrees of freedom that can be varied to optimize crystal packing and any functional groups present are in closer proximity. Looking at the chemical line drawing of $C_{13}Cl_9$ one might expect that prediction of the structure using one of the computer codes available would be successful, but currently available algorithms for crystal-structure prediction (see Lommerse *et al.*, 2000) would almost certainly fail to find the observed structure of $C_{13}Cl_9$ and would probably have substantial difficulty distinguishing between the closely related possible structures shown in Fig. 9.

This work was supported by the Office of Basic Energy Sciences, Department of Energy, under Grant No. DE-FG02-97ER45668.

References

Allen, F. H. & Kennard, O. (1993). *Chem. Des. Autom. News*, **8**, 1, 31–37.

Allen, F. H., Kennard, O., Watson, D. G., Brammer, L., Orpen, A. G. & Taylor, R. (1987). *J. Chem. Soc. Perkin Trans. 2*, pp. S1–S19.

Altomare, A., Cascarano, G., Giacovazzo, C., Guagliardi, A., Burla, M. C., Polidori, G. & Camalli, M. (1994). *J. Appl. Cryst.* **27**, 435–436.

Brock, C. P. & Dunitz, J. D. (1994). *Chem. Mater.* **6**, 1118–1127.

Coppens, P. (1967). *Science*, **158**, 1577–1579.

Coppens, P. & Sabine, T. M. (1968). *Molec. Cryst.* **3**, 507–512.

Dinnebier, R. E., Behrens, U. & Olbrich, F. (1997). *Organometallics*, **16**, 3855–3858.

Dinnebier, R. E., Schneider, M., van Smaalen, S., Olbrich, F. & Behrens, U. (1999). *Acta Cryst.* B**55**, 35–44.

Dunitz, J. D. & Gavezzotti, A. (1999). *Acc. Chem. Res.* **32**, 677–684.

Frisch, M. J., Trucks, G. W., Schlegel, H. B., Scuseria, G. E., Robb, M. A., Cheeseman, J. R., Zakrzewski, V. G., Montgomery, J. A. Jr, Stratmann, R. E., Burant, J. C., Dapprich, S., Millam, J. M., Daniels, A. D., Kudin, K. N., Strain, M. C., Farkas, O., Tomasi, J., Barons, V., Cossi, M., Cammi, R., Mennucci, B., Pomelli, C., Adamo, C., Clifford, S., Ochterski, J., Petersson, G. A., Ayala, P. Y., Cui, Q., Morokuma, K., Malick, D. K., Rabuck, A. D., Raghavachari, K., Foreman, J. B., Cioslowski, J., Ortiz, J. V., Stefanov, B. B., Liu, G., Fox, D. J., Keith, T., Al-Laham, M. A., Peng, C. Y., Nanayakkara, A., Wong, M. W., Andres, J. L., Gonzalez, C., Head-Gordon, M., Repogle, E. S. & Pople, J. A. (1998). *Gaussian*98, Revision A:6. Gaussian Inc., Pittsburgh, PA.

Gerson, F. (1966). *Helv. Chim. Acta*, **49**, 1463–1467.

Goto, K., Kubo, T., Yamamoto, K., Nakasuji, K., Sato, K., Shiomi, D., Takui, T., Kubota, M., Kobayashi, T., Yakusi, K. & Ouyang, J. (1999). *J. Am. Chem. Soc.* **121**, 1619–1620.

Haddon, R. C. (1975*a*). *Nature (London)*, **256**, 394–396.

Haddon, R. C. (1975*b*). *Aust. J. Chem.* **28**, 2343–2351.

Haddon, R. C. (1993). *Science*, **261**, 1545–1550.

Haddon, R. C., Chichester, S. V., Stein, S. M., Marshall, J. H. & Mujsce, A. M. (1987). *J. Org. Chem.* **52**, 711–712.

Haddon, R. C., Wudl, F., Kaplan, M. L., Marshall, J. H., Cais, R. E. & Bramwell, F. B. (1978). *J. Am. Chem. Soc.* **100**, 7629–7633.

Hazell, A. C. (1978). *Acta Cryst.* B**34**, 466–471.

Hazell, A. C. & Jagner, S. (1976). *Acta Cryst.* B**32**, 682–686.

Herbstein, F. H. (1979). *Acta Cryst.* B**35**, 1661–1670.

Kitaigorodskii, A. I. (1961). *Organic Chemical Crystallography*, pp. 130–138. New York: Consultant’s Bureau.

Koutentis, P. A., Chen, Y., Cao, Y., Best, T. P., Itkis, M. E., Beer, L., Oakley, R. T., Cordes, A. W., Brock, C. P. & Haddon, R. C. (2001). *J. Am. Chem. Soc.* **123**, 3864–3871.

Lommerse, J. P. M., Motherwell, W. D. S., Ammon, H. L., Dunitz, J. D., Gavezzotti, A., Hofmann, D. W. M., Leusen, F. J. J., Mooij, W. T., Price, S. L., Schweizer, B., Schmidt, M. U., Eijck, B. P. v., Verwer, P. & Williams, D. E. (2000). *Acta Cryst.* B**56**, 697–714.

Mackay, S., Gilmore, C. J., Edwards, C., Tremayne, M., Stuart, N. & Shankland, K. (1998). *maXus.* University of Glasgow, Scotland; Nonius BV, Delft, The Netherlands; MacScience Co. Ltd, Yokohama, Japan.

Mootz, D. & Wussow, H.-G. (1981). *J. Chem. Phys.* **75**, 1517–1522.

More, M., Baert, F. & Lefebvre, J. (1977). *Acta Cryst.* B**33**, 3681–3684.

Nonius (1999). *Collect.* Nonius BV, Delft, The Netherlands.

Otwinowski, Z. & Minor, W. (1997). *Methods Enzymol.* **276**, 307–326.

Overell, J. S. W. & Pawley, G. S. (1982). *Acta Cryst.* B**38**, 1966–1972.

Pauling, L. (1960). *The Nature of the Chemical Bond.* Ithaca, New York: Cornell University Press.

Prasad, S. M., Rae, A. I. M., Hewat, A. W. & Pawley, G. S. (1981). *J. Phys. C*, **14**, L929–L931.

Sheldrick, G. M. (1990). *SHELXTL PC.* Siemens Analytical Instruments Inc., Madison, Wisconsin, USA.

Sheldrick, G. M. (1997). *SHELXL97.* University of Göttingen, Germany.

Smaalen, S. van (1995). *Crystallogr. Rev.* **4**, 79–202.

Williams, J. H., Cockcroft, J. K. & Fitch, A. N. (1992). *Angew. Chem. Int. Ed. Engl.* **31**, 1655–1657.

Xia, A., Selegue, J. P., Carrillo, A., Patrick, B. O., Parkin, S. & Brock, C. P. (2001). *Acta Cryst.* B**57**, 507–516.